Unsteady hydraulic simulation of the cavitating part load vortex rope in Francis turbines

IOP Conf. Series: Journal of Physics: Conf. Series **813** (2017) 012020 doi:10.1088/1742-6596/813/1/012020

Unsteady hydraulic simulation of the cavitating part load vortex rope in Francis turbines

J Brammer[1], C Segoufin[1], F Duparchy[1], P Y Lowys[1], A Favrel[2], F Avellan[2]

[1]GE Renewable Energy, Hydro Solutions, 82 Avenue Léon Blum – BP75, 38041 Grenoble Cedex 9, France
[2]EPFL Laboratory for Hydraulic Machines, Avenue de Cour 33 bis, 1007 Lausanne, Switzerland

E-mail: james.brammer@ge.com

Abstract. For Francis turbines at part load operation a helical vortex rope is formed due to the swirling nature of the flow exiting the runner. This vortex creates pressure fluctuations which can lead to power swings, and the unsteady loading can lead to fatigue damage of the runner. In the case that the vortex rope cavitates there is the additional risk that hydro-acoustic resonance can occur. It is therefore important to be able to accurately simulate this phenomenon to address these issues. In this paper an unsteady, multi-phase CFD model was used to simulate two part-load operating points, for two different cavitation conditions. The simulation results were validated with test-rig data, and showed very good agreement. These results also served as an input for FEA calculations and fatigue analysis, which are presented in a separate study.

1. Introduction

The stochastic nature of production of new renewable energy technologies such as wind and photovoltaic has created the need for hydro power plants to be operated in a more flexible way to stabilise the grid. For Francis turbines, this increases number of hours at off-design conditions. At part load operation – typically between 50 % and 85 % of the optimal power of the turbine, the flow exiting the runner and, therefore, entering the draft tube has an increasing tangential component. This swirling flow creates instability in the flow field, and thus a helical vortex rope is formed in the draft tube cone. This vortex rope induces pressure fluctuations that can not only cause power swings but also increase fatigue loading on turbine components due to dynamic stresses. This vortex rope exists regardless of the presence of cavitation – however as already identified in the model tests conducted as a part of the Hyperbole project, the level of cavitation can have a dramatic effect on the pressure fluctuation levels as the natural frequency of the hydraulic circuit changes [1]. In a worst-case scenario, the excitation frequency of the vortex rope can match with the natural frequency of the test platform, and a resonance may occur. The same phenomena may occur on the power plant for possibly a different cavitation level and where the resonance can reach in rare cases an elevated level.

To study the part load vortex rope two operating points were identified. These have been named PL1 (corresponding to 80 % optimum discharge) and PL2 (corresponding to 64 % optimum discharge) respectively. Both were at rated head, and two different cavitation (sigma) numbers were chosen to study the influence of cavitation, as well as the accuracy of the CFD.

2. Single-phase calculations

2.1. Numerical setup

The part load vortex rope is a low frequency phenomenon – the rotation frequency is typically around $0.25 \cdot f_0$, where f_0 is the runner rotation frequency. Therefore, to have at least 10 revolutions of the vortex rope 40 runner revolutions are required. This necessitates a very large number of iterations during the CFD simulations. To achieve these numerical simulations in a practical timeframe a simplified computation domain was used. This domain neglected the spiral case and distributor. Instead a single guide vane was modelled upstream of the runner, using a prescribed flow angle at the domain inlet, and it was assumed that the flow was identical in each guide vane channel. The total number of mesh nodes used was 7.3 M (4.3 M in draft tube, 2.8 M in the runner and 0.2 M in the guide vane domain). To connect the guide vane domain with the runner, a stage interface therefore had to be used. This interface provides a circumferentially averaged flow field to the runner inlet, and therefore no effect of Rotor-Stator-Interaction (RSI) was modelled. This simplification was deemed acceptable for this analysis as the vortex rope is the main source of excitation at part load. This simplification not only dramatically reduced the total mesh size, but by not modelling the RSI a larger time step could be used; this was necessary to simulate a long enough time to ensure convergence. The runner and the draft tube domains were coupled using a transient-rotor-stator interface. The mass flow rate was specified at the inlet of the guide vane domain, along with a constant flow angle. At the outlet of the draft tube a constant static pressure was applied. All wall conditions were set using a no-slip condition and a smooth roughness model. The SAS-SST turbulence model was selected. The time step used was equivalent to half a blade passage of rotation. This is a rather large value; it was however deemed sufficient due to the domain simplification previously described.

2.2. Results

Initially a high cavitation number (sigma = 0.38) was investigated, where no cavitation was observed on profiles during the model test, and therefore single phase CFD could be used. The results showed discrepancies in prediction of both the torque and head values. This is mainly due to the spiral case and distributor not being considered, but also could be improved with mesh refinement. However, as the purpose of the study was to investigate the part load vortex rope, the velocity profiles in the draft tube cone were also compared with LDV measurements [2] in order to confirm that from a hydraulic perspective the correct operating point was being modelled.

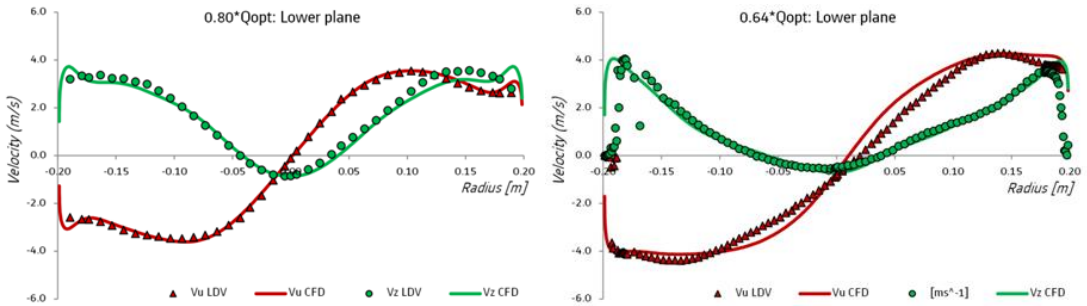

Figure 1: Time-averaged velocity profiles in the draft tube cone
(red series = circumferential velocity, green series = axial velocity, solid line = CFD, Points = LDV measurements)

This comparison is shown in Figure 1 for both part load operating points. An excellent agreement is observed between the CFD and experimental results, which confirms that the correct operating point was being modelled with a reasonable level of accuracy. It is also interesting to note that both the experimental and CFD results show a slight asymmetry in the flow field. The pressure fluctuations in the runner and draft tube were then analysed. Virtual pressure sensors were placed in the CFD model, in the same positions as on the scale model used for experimental measurements on the test rig. This included multiple sensors in the draft tube cone, elbow and liner, as well as on the runner blades.

Figure 2 shows the results for a sensor placed in the draft tube cone for both operating points. Comparing the CFD predictions with the experimental measurements a very good correlation is observed, the form of the time series matches well with the measurements, suggesting that the dynamics of the vortex rope is well predicted. The experimental signals show a higher frequency content, which was not expected in the simulation due to the relatively large time step used, and to the fact that the stage interface was used at the runner inlet.

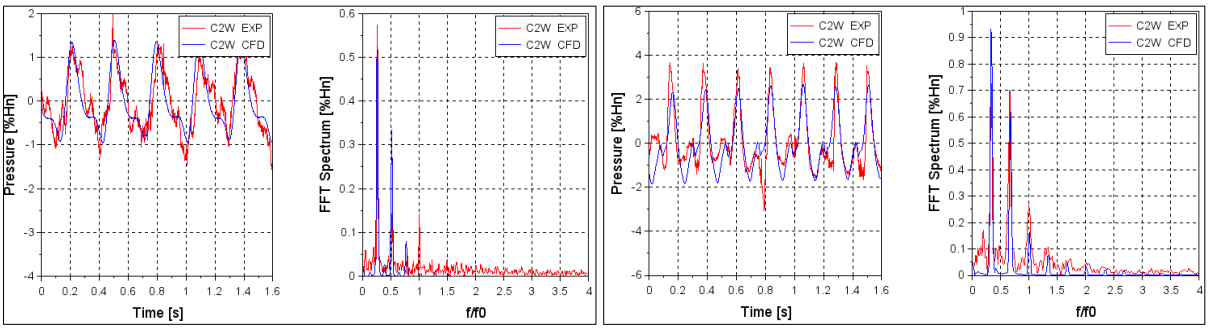

Figure 2: Pressure versus time and associated FFT analysis ($\Delta H_{RMS}/Hn$ %) for PL1 (left) and PL2 (right)

The pressure fluctuations measured by four rotating sensors mounted on the instrumented runner are shown in Figure 3. Two sensors were located on the pressure side of one blade close to the trailing edge and two others located on the suction side of one blade close to the trailing edge. Looking at the results the CFD and experimental frequencies match, and the low frequency fluctuations are the signature of the part load vortex rope. The CFD does however appear to under predict the magnitude of the pressure fluctuations on the runner blades.

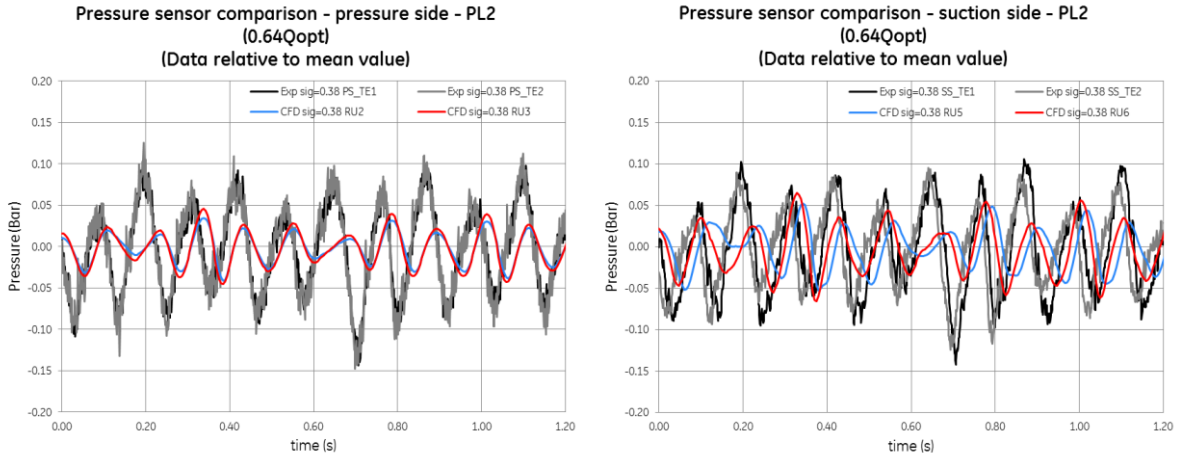

Figure 3: Pressure sensors mounted on the instrumented runner for PL2 (left: pressure side of blade, right: suction side of blade)

This is made more evident on the pressure side sensors (left graph) where the RSI signal values are higher. Therefore, it is likely that this under prediction of the pressure fluctuations is due to the stage interface, and the large time step used. Further analysis of the on-board sensor measurements is detailed in [3].

3. Multi-phase calculations

Complimentary studies of this runner have shown that the cavitation number has a significant influence on the pressure fluctuations throughout the hydraulic system [1], [4] and [5]. At sigma = 0.16 there is a dramatic increase in the level of pressure fluctuations despite the cavitation volume being smaller than

at the plant sigma condition (plant sigma = 0.12). This is due to the natural frequencies of the hydro-acoustic system and the turbine test-rig being equal at this point, and therefore resonance occurs. As this resonance is an interaction of the hydraulic circuit with the test rig circuit, it is not possible to model this phenomenon using only a CFD calculation of the single turbine, even with multiple phases. A representation of the test rig would be required in the simulation, and this could potentially be achieved by coupling a CFD calculation with a 1D hydro-acoustic model. Therefore, for the following CFD results this resonance point was avoided, and a cavitation number sigma = 0.12 was chosen, with this point corresponding to the plant value.

3.1. Numerical setup

The numerical setup was the same as the single-phase calculations, except that a multi-phase model was implemented and that the static pressure at the outlet was adjusted iteratively until the correct cavitation number was calculated. For this study the homogenous cavitation model was used [6], such that the two phases shared a common flow field. This was deemed appropriate given that the high flows in the turbine would dominate the advective processes. The two phases were defined as water and water vapour respectively. The phase-change process was modelled using the Rayleigh-Plesset model.

3.2. Results

Figure 4 shows a comparison of the visualized cavitating vortex rope and the CFD prediction. In the CFD calculation the vortex is visualized by two iso-volumes of the vapour volume fraction, with values of 10 % and 90 % used to capture the full extent of the cavitation volume. Comparing the two visualizations, the vortex rope has been well predicted in terms of the cavity shape. It was observed, by both CFD and the experiments, that as the vortex rope contacts the elbow wall, it collapses and travels upwards towards the runner.

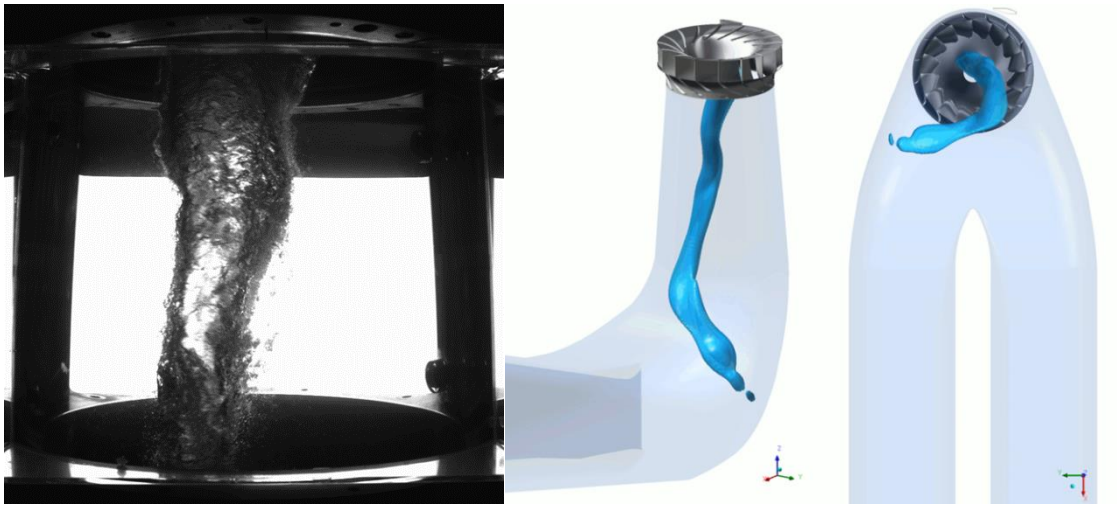

Figure 4: Comparing the observed vortex rope from laboratory observations (left) and CFD calculations (right).

The time-averaged values of the pressure fluctuations in the draft tube cone and on the runner are shown in Figure 5 for both cavitation conditions (i.e. sigma = 0.12 and 0.35). Both calculations show good agreement with the experimental results, with the FFT results showing good coherence. For sigma = 0.12 the cone sensors (left image) are particularly accurate, whereas for the embedded sensors the levels are slightly under predicted, as was the case for the first simulation in cavitation free conditions.

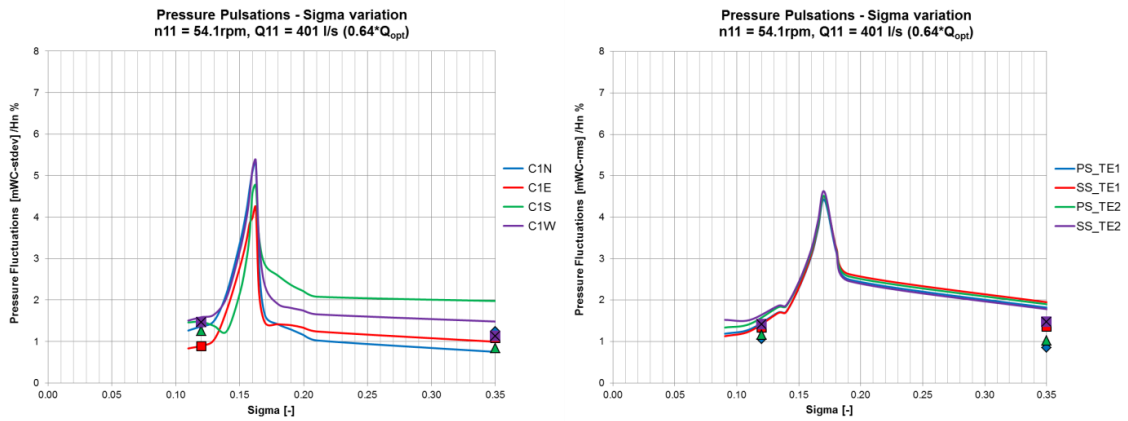

Figure 5: Cavitation number (sigma) influence on the pressure fluctuations ($\Delta H_{RMS}/Hn$ %) in the cone (left) and rotating sensors mounted on the instrumented runner (right) for PL2– Points are CFD results, line series are experimental data

4. Conclusion

Single and multi-phase CFD calculations were launched to investigate the part load cavitation vortex rope. The results were validated with standard integral values, LDV flow field surveys, and wall pressure sensors both on the stationary parts of the turbine model as well as the runner, all of which were measured as part of the Hyperbole project.

For the case of hydro-acoustic resonance, the current methodology is not able to capture this phenomenon as the entire hydraulic circuit would need to be modelled [7], therefore two sigma values were chosen outside of this resonance – The first one at sigma = 0.38 and the second one at sigma = 0.12, which corresponds to the plant value.

A simplified computational domain was used to reduce the CPU time. The CFD predictions showed an excellent correlation with the experimental test rig measurements and was therefore capable to predict the complex phenomena of the part load vortex rope outside of the resonance condition.

The influence of the cavitation number had little effect on the pressure fluctuations, and therefore a single-phase simulation would have been sufficient to predict the dynamic loads. However, other operating conditions may need to use multi-phase models if the phenomena are dependent on cavitation. This type of calculation allows us to not only gain an understanding of the hydraulic behaviour at off-design conditions, but can also serve as an input to mechanical calculations so that the fatigue and runner lifetime can be evaluated [8].

Acknowledgments

The research leading to the results published in this paper is part of the HYPERBOLE research project, granted by the European Commission (ERC/FP7- ENERGY-2013-1-Grant 608532).

References

[1] Favrel, A., Müller, A., Landry, C., Yamamoto, K. and Avellan, F., Experiments in Fluids, vol. 56(12), 2015. doi:10.1007/s00348-015-2085-5.
[2] Favrel, A., Müller, A., Landry, C., Yamamoto, K. and Avellan, F., Experiments in Fluids, vol. 57(11), 2016. doi: 10.1007/s00348-016-2257-
[3] Duparchy, F., Favrel, A., Lowys, P.Y., Landry, C., Müller, A., Yamamoto, K. and Avellan, F., 2016 Journal of Physics: Conference Series 656 012061 (CAV2015, Lausanne, Switzerland)
[4] Müller A., Dreyer M., Andreini N. and Avellan F., Experiments in Fluids, vol. 54, num. 4, p. 1-11, 2013.
[5] Yamamoto, K., Müller, A., Favrel, A et al. 2014, In IOP Conference Series: Earth and Environmental Science (Vol. 22, No. 2, p. 022011). IOP Publishing.
[6] ANSYS CFX, Release 16.0, ANSYS CFX-Solver Theory Guide, Chapter 5: Multiphase Flow Theory.
[7] Landry, C., Favrel, A., Müller, A., Nicolet, C., Yamamoto, K. and Avellan, F., 27th IAHR Symposium on Hydraulic Machines and Systems in *IOP Conf. Ser.: Earth Environ. Sci.* 22 032037, 2014.
[8] Brammer, J., Duparchy, F., Lowys P.Y., Thibaud, M, Wheeler, K. and de Colombel, T., "*Increasing the operating range of Francis turbine by considering dynamic phenomena at partial load*", Hydro 2016, Montreux, Switzerland.